Oncogene (2003) 22, 3875–3887

www.nature.com/onc

Activation of β-catenin in prostate epithelium induces hyperplasias and squamous transdifferentiation

Brian Bierie[1,7], Masahiro Nozawa[1,7], Jean-Pierre Renou[1,2], Jonathan M Shillingford[1], Fanta Morgan[1], Takami Oka[1], Makoto M Taketo[3], Robert D Cardiff[4], Keiko Miyoshi[1,5], Kay-Uwe Wagner[6], Gertraud W Robinson[1] and Lothar Hennighausen*[,1]

[1]*Laboratory of Genetics and Physiology, National Institute of Diabetes and Digestive and Kidney Diseases, National Institutes of Health, Bethesda, MD 20892, USA;* [2]*Institut National de la Recherche Agronomique, Jouy-en-Josas Cedex, France;* [3]*Department of Pharmacology, Kyoto University Graduate School of Medicine, Sakyo, Kyoto 606-8501, Japan;* [4]*Center for Comparative Medicine, University of California, Davis, CA 95616, USA;* [5]*Department of Biochemistry, School of Dentistry, The University of Tokushima, Tokushima 770-8504, Japan;* [6]*Eppley Institute for Research in Cancer and Allied Diseases, University of Nebraska Medical Center, Nebraska Medical Center, Omaha, Nebraska*

The Wnt/β-catenin signaling pathway is critical for normal mammalian development, the specification of epidermal cells and neoplastic transformation of intestinal epithelium. However, precise molecular information regarding cell-specific responses to β-catenin signaling has been limited. This question was addressed using a mouse model in which exon 3 of the β-catenin gene was deleted in several cell types with loxP-mediated recombination utilizing a Cre transgene under control of the mouse mammary tumor virus-long terminal repeat (MMTV-LTR). The stabilization of β-catenin in prostate epithelium resulted in hyperplasias and extensive transdifferentiation into epidermal-like structures, which expressed keratins 1 and 6, filaggrin, loricrin and involucrin. The cell-specific loss of NKCC1 protein and reduced nuclear Stat5a is further suggestive of a loss of prostate epithelial characteristics. In addition to the prostate, hyperplasias and squamous metaplasias were detected in epithelia of the epididymis, vas deferens, coagulating gland, preputial gland and salivary gland. However, and in contrast to a recent study, no lesions reminiscent of high-grade prostate intraepithelial neoplasia were detected. Since β-catenin was activated in several cell types and impinged upon the viability of these mice, it was not possible to evaluate the cumulative effect over more than 3 months. To assess long-term consequences of β-catenin activation, mutant and control prostate tissues were transplanted into the mammary fat pads of wild-type males. Notably, squamous metaplasias, intra-acinous hyperplasia and possible neoplastic transformation were observed after a total of 18 weeks of β-catenin stimulation. This suggests that the transdifferentiation into squamous metaplasias is an early response of endoderm-derived cells to β-catenin, and that the development of intra-acinous hyperplasias or neoplastic foci is a later event.

Oncogene (2003) **22,** 3875–3887. doi:10.1038/sj.onc.1206426

Keywords: β-catenin; cell identity; transdifferentiation; neoplasia; prostate

Introduction

β-Catenin is an integral part of the Wnt signaling pathway and has been linked to developmental processes including cell fate specification, polarity and migration (McCrea *et al*., 1991; Gat *et al*., 1998; Brault *et al*., 2001; Merrill *et al*., 2001; Niemann *et al*., 2002). Wnt proteins bind to Frizzled receptors and induce a signaling cascade that leads to the stabilization of β-catenin. The stabilized β-catenin is able to interact with the lymphoid enhancer transcription factors (LEFs) and T-cell factors (TCFs), which subsequently activate genetic programs (Roose *et al*., 1999; de Lau and Clevers, 2001; Hovanes *et al*., 2001). Genetic loss and gain of function experiments (Haegel *et al*., 1995; Gat *et al*., 1998; Huelsken *et al*., 2000, 2001; Widelitz *et al*., 2000) have revealed the importance of β-catenin in the determination of the anterior–posterior axis and mesoderm structures during fetal development, and its role in the specification of cell fate. Furthermore, β-catenin signaling is essential for the follicular differentiation of epidermal cells and the expression of a stabilized β-catenin in these cells results in the formation of unscheduled hair follicles (Gat *et al*., 1998). In support of this observation, an epidermal fate is adopted by stem cells in the skin in the absence of β-catenin (Huelsken and Birchmeier, 2001; Huelsken *et al*., 2001). Such lineage decisions appear to be regulated through specific genetic programs initiated by TCF3/LEF complexes (Merrill *et al*., 2001). Recently, we demonstrated that the stabilization of β-catenin in differentiated mammary epithelium results in a loss of differentiation and the

*Correspondence: L Hennighausen, Laboratory of Genetics and Physiology, NIDDK, NIH Building 8, Room 101, Bethesda, MD 20892-0822, USA; E-mail hennighausen@nih.gov
[7]Both contributed equally to this work
Received 29 July 2002; revised 28 January 2003; accepted 28 January 2003

transdifferentiation into epidermal-like structures (Miyoshi *et al*., 2002a), further demonstrating the ability of this signaling pathway to determine cell fate.

Aberrant signaling through β-catenin has been found in many tumors, in particular those of the colon (e.g. Polakis, 2000). Mutations in the β-catenin pathway have been observed in approximately 5% of human prostate cancers (Voeller *et al*., 1998; Chesire *et al*., 2000) and there is evidence to suggest that aberrant β-catenin signaling contributes to prostate growth and tumorigenesis (Chesire *et al*., 2002; Gerstein *et al*., 2002). To establish whether tumorigenesis in the prostate can be induced by activated β-catenin alone, mice ($Catnb^{+/lox(ex3)}$) were generated (Harada *et al*., 1999) that express stabilized β-catenin in prostate epithelium upon Cre-mediated excision of exon 3 (amino acids 5–80). Deletion of exon 3 in several cell types, including prostate epithelium, vas deferens, coagulating gland, preputial gland, basal cells in skin and salivary epithelium, was achieved through the use of transgenic mice that carry the Cre gene under the control of the MMTV-LTR (Wagner *et al*., 1997, 2001). To determine the cellular changes induced by β-catenin immunohistochemical approaches and microarray analyses were used to identify proteins and genes, respectively, whose expressions were altered.

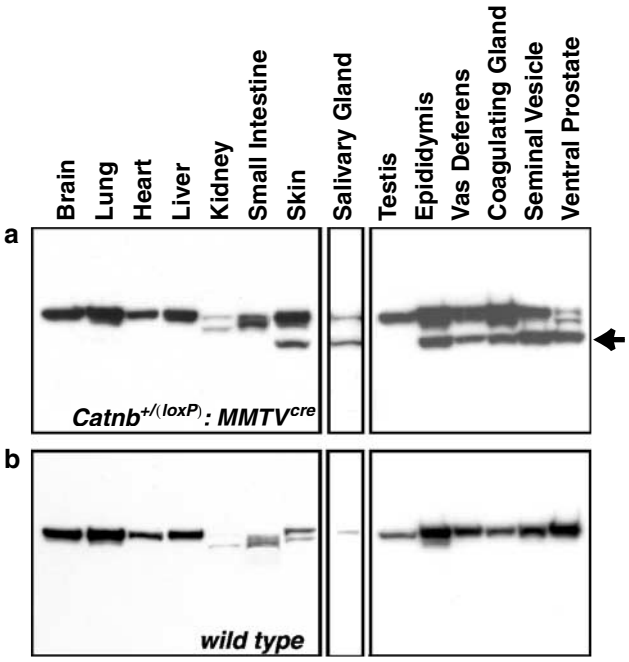

Figure 1 Expression of stabilized β-catenin in $Catnb^{+/\Delta ex3}$:$MMTV^{cre}$ mice. Proteins were extracted from different tissues types of 8-week-old $Catnb^{+/\Delta ex3}$:$MMTV^{cre}$ mice (**a**) and age-matched littermate controls (**b**). Stabilized β-catenin was detected in skin, salivary gland, epididymis, vas deferens, coagulating gland, seminal vesicle and the ventral prostate (arrow)

Results

Stabilization of β*-catenin in different tissues*

Exon 3 of the β-catenin gene (amino acids 5–80) encodes critical serine and threonine residues that, upon phosphorylation, target the β-catenin protein for ubiquitin-mediated degradation. Mice have been generated that carry exon 3 of the β-catenin gene flanked by loxP sites. Using these mice, it has been demonstrated that Cre-mediated loss of exon 3 specifically in the intestine results in the generation of a truncated stabilized β-catenin and the formation of intestinal polyposis (Harada *et al*., 1999). To further assess the consequence of β-catenin stabilization in other cell types, the conditionally targeted β-catenin mice were crossed with a mouse line expressing the Cre transgene under the control of the MMTV-LTR (Wagner *et al*., 1997, 2001), which is referred to as $Catnb^{+/\Delta ex3}$:$MMTV^{cre}$ mice

$Catnb^{+/\Delta ex3}$:$MMTV^{cre}$ mice could be identified visually at 10 days of age because they exhibited sparse and irregular hair growth (data not shown). In addition, these mice developed thickness of the eyelids, nose and ears within 6 weeks after birth (data not shown). An increase in the number of hair follicles and the presence of epithelioid cysts was observed (data not shown) similar to transgenic mice expressing stabilized β-catenin under the control of a K14 promoter (Gat *et al*., 1998). To monitor the deletion of exon 3, the appearance of truncated β-catenin protein was analysed by way of western blots. As shown in Figure 1, β-catenin was present in all tissues examined. The truncated form of β-catenin was evident in skin, salivary gland, epididymis, vas deferens, coagulating gland, seminal vesicle, ventral prostate (Figure 1a), spleen and mammary tissue (data not shown) of $Catnb^{+/\Delta ex3}$:$MMTV^{cre}$ mice. The appearance of N-terminal truncated β-catenin in these tissues is consistent with the cell-specificity of Cre activity in MMTV-Cre transgenic mice (Wagner *et al*., 2001).

Stabilization of β*-catenin causes hyperproliferation and squamous transdifferentiation of prostate epithelium*

Histological analysis of the ventral prostate from $Catnb^{+/\Delta ex3}$:$MMTV^{cre}$ mice at 8 weeks of age revealed papillary epithelial hyperplasias and evidence of epithelial cells growing into the ductal lumina (Figure 2a). Some ducts were filled with epithelial cells (Figure 2a) and also contained extensive squamous metaplasias (Figure 2b), which were similar to those observed in the mammary tissue expressing stabilized β-catenin (Miyoshi *et al*., 2002a). Furthermore, comparable to mammary tissue, the early lesions were characterized by an abundance of ghost cells (Figure 2b). Prostate tissue from littermates that did not carry the Cre transgene exhibited normal histology consisting of regular acini and ducts and normal nuclei (Figure 2c). By 12 weeks of age, the majority of prostate epithelium had undergone squamous transdifferentiation (Figure 2d and e). Extensive transdifferentiation was also observed in the preputial gland (Figure 2f).

Tissue from eight mutant mice was examined (7.5–12 weeks of age) and all sampled lobes of the prostate and

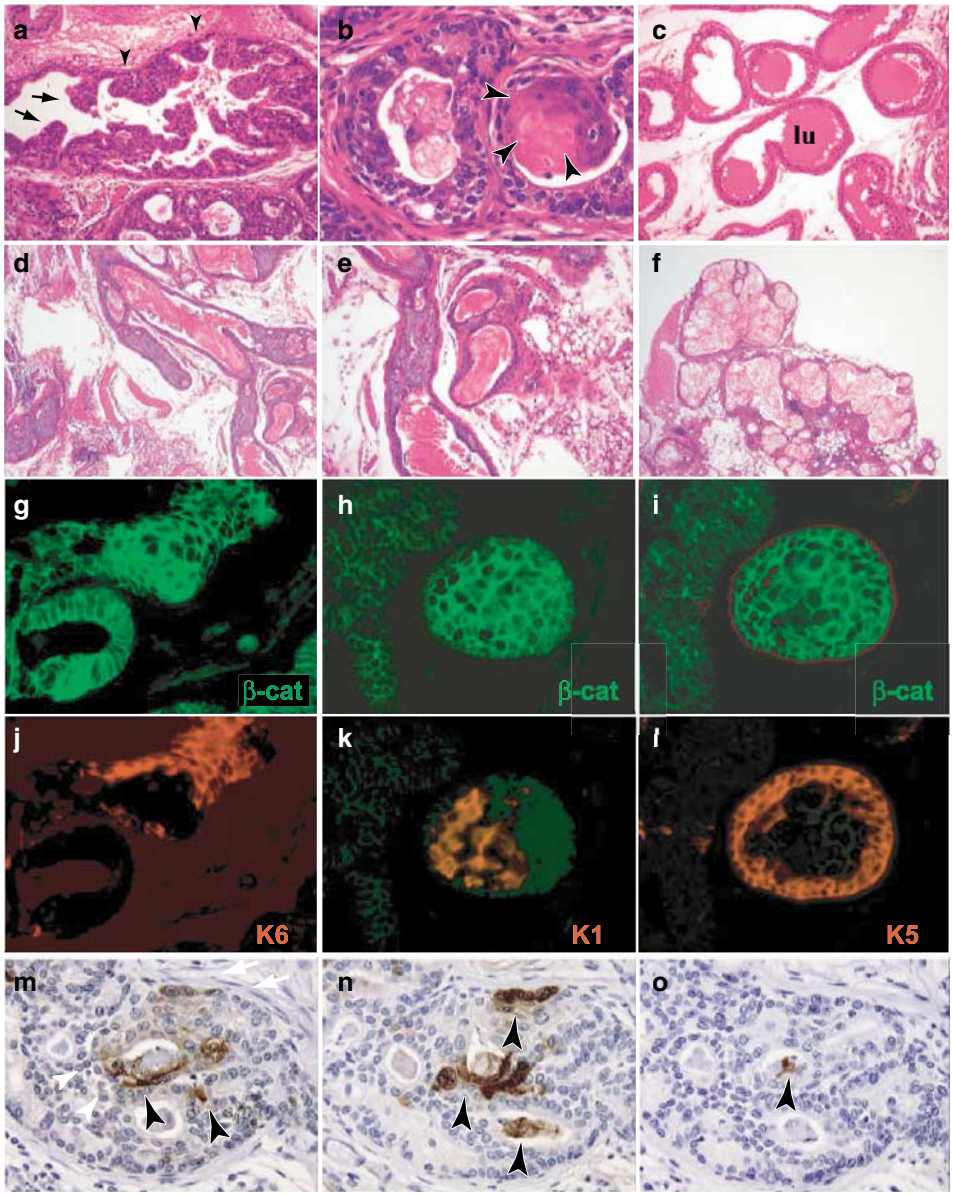

Figure 2 Hyperplasias and squamous metaplasia in prostate epithelium of mutant mice. (**a**–**c**) Hematoxylin and eosin (H&E) staining of the ventral prostate from 8-week-old *Catnb*$^{+/\Delta ex3}$*:MMTV*^{cre} (**a** and **b**) and wild-type (**c**) mice. Epithelial hyperplasias were observed (arrows in panel a), and the basement membrane was intact (arrowheads). Arrowheads in panel b, squamous metaplasias. (**d**) Squamous metaplasias in prostate tissue from a 12-week old mutant mouse showing areas of extensive squamous transdifferentiation. (**e**) Higher magnification of a keratinized area shown in (**d**). (**f**) Squamous metaplasia in the preputial gland. (**g**–**l**) Immunohistochemistry of β-catenin (**g**–**i**) with keratin 6 (**j**), keratin 1 (**k**), keratin 5 (**l**) and late differentiation markers of epidermis, loricrin (**m**), involucrin (**n**), filaggrin (**o**) in the ventral prostate from 8-week-old *Catnb*$^{+/\Delta ex3}$*:MMTV*^{cre} mice. (**j**) Keratin 6 was highly expressed in cells close to those expressing accumulated β-catenin (**g**) in hyperplastic lesions. (**k**) Keratin 1 was detected in cells that were localized within the squamous metaplasias. (**l**) Keratin 5 expression was observed not only in the single layer surrounding the acini but also in more centralized cells close to squamous metaplasias. (**m** and **n**) Loricrin and involucrin were expressed extensively (arrow heads). (**o**) Filaggrin was sporadically expressed (arrowhead). Magnification: (**a**–**c**), ×200; (**g**–**m**), ×630

submucosal glands of the internal urethra were involved with a diffuse proliferative process of the epithelium. This process was associated with a diffuse interstitial infiltrate of lymphocytes and plasma cells (chronic inflammation). Loss of normal differentiation of the prostatic epithelium was observed and the glands were filled with highly mitotic densely crowded cells that had large, slightly pleomorphic hyperchromatic nuclei with relatively deficient cytoplasm. As the glands became filled with cells, the epithelium developed distinct multiple layers and formed back-to-back (cribriform) structures within the ducts. The most striking element was the tendency to form small foci of multilayered squamous cells. These foci were associated with the production of keratin swirls and hyalinized hard keratin. Keratohyalin granules were seen in the cytoplasm of

some of these foci. The keratinization, however, was very abrupt without a granular layer.

To establish on a molecular level whether the prostate epithelium had undergone a transdifferentiation process and acquired epidermal markers, immunohistochemistry was performed with antibodies against keratin 1, keratin 5 and keratin 6 as well as β-catenin. While keratin 1 and keratin 6 were not expressed in prostate epithelium from wild-type mice (data not shown), keratin 5 was detected in the epithelial lining of acini and ducts (data not shown). This is consistent with the expression pattern of keratin 5 in human prostate (Achtstatter *et al*., 1985). In *Catnb*$^{+/\Delta ex3}$*:MMTV*^{cre} mice, however, keratin 6 was detected in cells with a close proximity to those overexpressing β-catenin (Figure 2j and g). Keratin 1 expression also coincided with elevated levels of β-catenin (Figure 2k and h), while keratin 5 was localized not only in the single layer of cells surrounding the acini but also in more central cells (Figure 2l and i), which was confirmed by serial sections. This pattern of keratin expression was similar to that observed in the β-catenin-induced transdifferentiation of mammary tissue, which we described previously (Miyoshi *et al*., 2002a). To further establish that prostate epithelium had acquired biochemical features of epidermal differentiation, the presence of filaggrin, loricrin and involucrin was established. Filaggrin is normally detected in the stratus corneum, loricrin in the granular layer and involucrin in the spinous layer of the skin (Fuchs and Byrne, 1994). While no expression was observed in normal prostate tissue (data not shown), extensive expression of loricrin and involucrin (Figure 2m and n), but not filaggrin (Figure 2o), was observed in prostate tissue upon the stabilization of β-catenin. Taken together, and in agreement with the previous study in the mammary gland (Miyoshi *et al*., 2002a), detection of several epidermal markers provides compelling evidence that the continuous presence of β-catenin in prostate epithelium results in the transdifferentiation into epidermal-like structures.

Identification of genes deregulated upon the stabilization of β*-catenin*

To identify genes that are either induced or repressed upon the stabilization of β-catenin, we monitored gene expression using cDNA microarrays. The 12.6k microarray contained genes from the NCI oncochip (GEM1) and all of the clones from the LGP mammochip (Miyoshi *et al*., 2002b). RNA was prepared using prostates from four 8-week-old transgenic mice and four control littermates, labeled and used for hybridization. Out of the 12 600 on the array, 92 genes were differentially expressed with a ratio of three-fold or greater (51 were higher in the transgenic mice and 41 were lower). Out of those, 24 were known genes and 68 were unknown ESTs (Table 1). Interestingly, expression of eight genes, including IMAGE clones 1493858, 947821, 1511503, 1382204, 1348833 and 1246820 were induced not only in prostate epithelium upon stabilization of β-catenin, but also in squamous metaplasias observed in the mammary epithelium following β-catenin stabilization (Renou *et al*., submitted).

To determine whether expression of these differentially regulated genes was linked to specific cell types and the development of neoplasias, the entire EST database containing in excess of 2 000 000 clones was screened. NKCC1 and lactotransferrin were found predominantly in cDNA libraries from neoplastic mammary tissue, whereas expression of SPRR2A was largely confined to colon libraries. A total of 50 matches were found for

Table 1 Filtered microarray results for Δex3 and wt prostate

Image clone	*Gene*	*Ratio*
IMAGE:874383	: lactotransferrin	9.41
IMAGE:440344	: glutamine synthetase	7.20
IMAGE:888512	: small proline-rich protein 2A	7.13
IMAGE:580715	: lymphocyte antigen 6 complex, loc. A	6.57
IMAGE:493658	: lipocalin 2	6.30
IMAGE:777018	: selenoprotein	6.25
IMAGE:570673	: cytoskeletal crystallin	5.67
IMAGE:697864	: peptidoglycan recognition protein	5.28
EST	: IMAGE:1493858, 1400033, 721906, 752174, 419553, 425482, 420322, 6200655, 418861, 418440, 407068, 904900, 1382204, 803309, 751826, 427469	
IMAGE:579391	: carbonic anhydrase 2	4.72
IMAGE:1396803	: WM65 kappa immunoglobulin	4.61
IMAGE:425855	: lymphocyte antigen 6 complex, loc. C	3.85
IMAGE:467107	: procollagen, type V, alpha 2	3.75
IMAGE:418564	: similar to KIAA0405	3.55
IMAGE:874833	: extracellular matrix protein 1	3.40
EST	: IMAGE:350088, 596604, 597005, 948984, 832620, 1246820, 947821, 440564, 676176, 820179, 949686, 808780, 888577, 634753, 420323, 1348833, 720566, 617816, 949074	
IMAGE:751710	: Net 1	2.71
IMAGE:1382855	: amyloid beta (A4) precursor-like protein 2	2.59
IMAGE:522713	: major urinary protein 1	0.33
IMAGE:480620	: procollagen, type VI, alpha 3	0.32
IMAGE:736616	: laminin, alpha 4	0.30
IMAGE:849511	: HELG	0.28
IMAGE:948373	: melanophilin	0.24
IMAGE:875502	: smooth muscle leiomodin	0.23
EST	: IMAGE:639215, 920069, 1448100, 832470, 807862, 735089, 657766, 1265663, 1247930, 440563, 477045, 596027, 1493894, 761718, 576459, 679563, 875422, 388008, 875246, 1195338, 765660, 850717, 749752	
IMAGE:466122	: solute carrier family 12, mb 2 (NKCC1)	0.18
IMAGE:466191	: calsequestrin 2	0.09
EST	: IMAGE:1397029, 474319, 889659, 832580, 832511, 481701, 550916, 1396267, 463092, 315676	

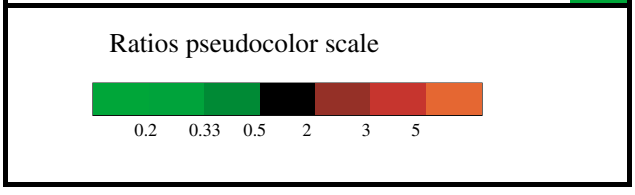

lactotransferrin, with 37 of them in a single library prepared using mammary hyperplasias from transgenic mice overexpressing TGFα in mammary epithelium (Humphreys and Hennighausen, 1999). These findings suggest that the expression of these genes is also associated with hyperplastic epithelium from other tissues and not confined to the hyperplastic transdifferentiating prostate. To verify the results from the microarray experiments, Northern blot analyses and immunohistochemistry were performed with several known genes, whose expression was induced in β-catenin transformed prostate tissue. RNA levels for lactotransferrin (LTF), small proline-rich protein 2A (SPRR2A), neuroepithelial cell transforming gene 1 (NET1) and amyloid beta precursor-like protein 2 (APLP2) were highly elevated in mutant prostate tissue, in agreement with the microarray data (Figure 3). Hybridization to GAPDH mRNA was used as a loading control.

Genes whose expression is altered in transdifferentiated tissue may not be under direct control of β-catenin, rather the deregulation might be a consequence of a changed ratio of cell types or an altered physiological state of the animal. In order to identify early physiological and transcriptional changes induced by stabilized β-catenin, a cell-based system was used that permitted a temporal activation of β-catenin. The deletion of exon 3 in mouse embryonic fibroblast (MEF) cultures from $Catnb^{+/\Delta ex3}$ mice was induced with a retrovirus-based Cre recombinase (Krempler *et al*., 2002). The presence of stabilized β-catenin was detected within 48 h after infection (Figure 4b, lane 4). RNA from $Catnb^{+/\Delta ex3}$ cells that had been infected with the retrovirus and RNA from $Catnb^{+/\Delta ex3}$ cells without retroviral infection were used for array analysis (Table 2). Out of 17 genes exhibiting significant changes in expression level, a total of 11 were induced upon β-catenin activation including the one encoding TGFβ2. None of the genes induced in the cell culture system were activated in the transdifferentiated prostate tissue. These results suggest that either the response to β-catenin is cell-specific or all of the changes that we have observed in the prostate are secondary effects of the transdifferentiation process or expressed by the invading inflammatory cell types.

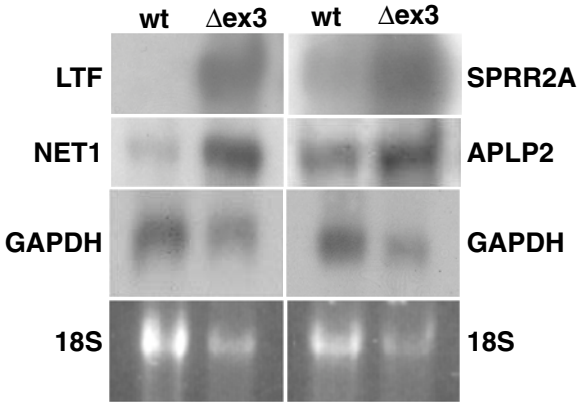

Figure 3 Northern blot confirmation of microarray analyses. Total RNA was purified from wild type (wt) and $Catnb^{+/\Delta ex3}$:$MMTV^{cre}$ (Δex3) prostate. Lactotransferrin, LTF; small proline-rich protein 2A, SPRR2A; neuroepithelial cell transforming gene 1, NET1; amyloid beta precursor-like protein 2, APLP2; and glyceraldehyde-3-phosphate dehydrogenase, GAPDH as a loading control

Stabilization of β*-catenin causes the loss of normal prostate epithelial characteristics*

Expression of several genes, including the gene encoding the sodium potassium chloride cotransporter NKCC1 was lower in mutant prostate as compared to wild-type prostate. The presence of NKCC1 has been linked to the differentiation status of mammary epithelium (Miyoshi *et al*., 2001; Shillingford *et al*., 2002a, b) and it can be hypothesized that the reduced expression upon stabilization of β-catenin was linked to a loss of differentiation. Immunohistochemical experiments established the presence of a homogeneous distribution of NKCC1 protein at the basolateral membrane of prostate epithelial cells in the wild-type animal (Figure 5b), similar to that observed in mammary epithelial cells in virgin mice (Shillingford *et al*., 2002b). In contrast, expression of NKCC1 in prostate epithelium from $Catnb^{+/\Delta ex3}$:$MMTV^{cre}$ mice was heterogeneous and its absence was associated with cells that exhibited elevated β-catenin levels (Figure 5a, a′ and a″). The observed reduction in NKCC1 expression supports the results of the microarray analyses, and the restricted loss of NKCC1 in areas of β-catenin activation supports the notion that these cells have lost their normal status of differentiation.

It has been proposed that the signal transducer and activator of transcription 5a (Stat5a) plays a critical role not only in mammary development (Liu *et al*., 1997; Miyoshi *et al*., 2001) but also in the maintenance of normal tissue architecture and function of the mouse prostate (Nevalainen *et al*., 2000). In this context, the stabilization of β-catenin resulted in the suppression of

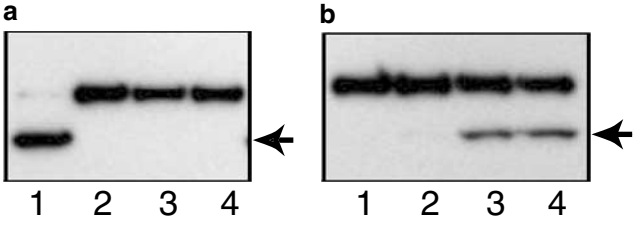

Figure 4 Western blot demonstrating the retro-Cre mediated deletion in $Catnb^{+/\Delta ex3}$ mouse embryonic fibroblasts (MEFs). The efficiency in recombination and production of stabilized β-catenin (**a**) was visualized through the appearance of a band representing the truncated protein after retro-Cre mediated recombination and selection (lane 1). Nontreated $Catnb^{\Delta ex3/\Delta ex3}$ MEFs (lane 2). WT MEFs after infection and selection (lane 3). WT noninfected control MEFs (lane 4). Excision of exon 3 in the $Catnb^{+/\Delta ex3}$ MEFs (**b**) resulted in a truncated stabilized β-catenin within 48 h after infection. Little recombination occurred by 12 or 24 h (lanes 1 and 2, respectively), but the truncated form of β-catenin (lower band) was evident at 36 and 48 h (lanes 3 and 4, respectively) after infection

Table 2 Filtered microarray results for Δex3 and wt MEFs

Image clone	: *Gene*	*Ratio*
IMAGE:477066	: four and a half LIM domains 1	**3.51**
IMAGE:367780	: transforming growth factor, beta 2, TGF 2	**3.50**
IMAGE:1248313	: ESTs	2.73
IMAGE:331186	: caveolin-1	2.53
IMAGE:596968	: caveolin-1	2.48
IMAGE:1383618	: ESTs	2.31
IMAGE:874923	: ESTs	2.23
IMAGE:493212	: hormone/GF hepar bind	2.16
IMAGE:948509	: caveolin-1	2.15
IMAGE:670830	: ESTs	2.09
IMAGE:421546	: ESTs	2.06
IMAGE:463207	: ESTs	0.40
IMAGE:354318	: pentaxin-related gene	0.37
IMAGE:1349911	: asporin	0.36
IMAGE:963845	: ESTs	0.33
IMAGE:478168	: pleiotrophin	0.30
IMAGE:580715	: lymphocyte antigen 6 complex, locus A	0.23

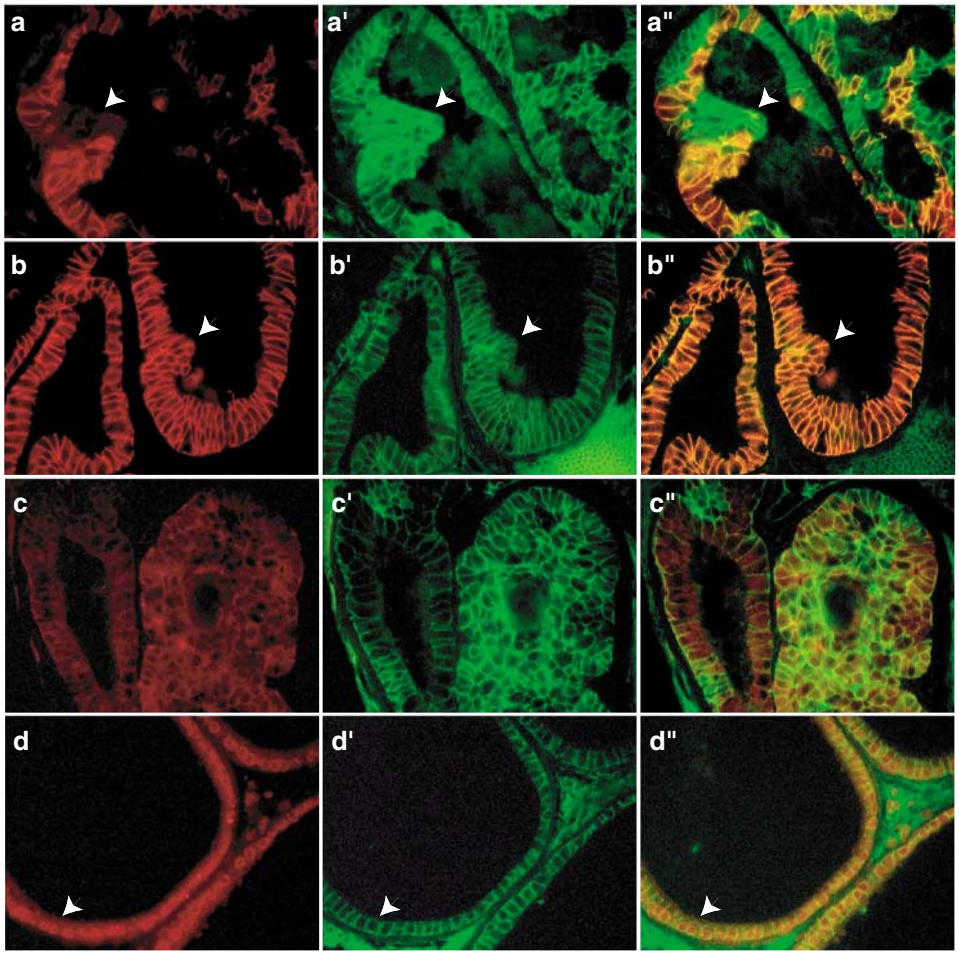

Figure 5 Stabilization of β-catenin caused hyperplasia with loss of NKCC1 and Stat5a expression in prostate epithelium. Immunohistochemistry of β-catenin with NKCC1 (**a** and **b**), and Stat5a (**c** and **d**) in the ventral prostate from 8-week-old $Catnb^{+/\Delta ex3}$;$MMTV^{cre}$ mice (**a** and **c**) and wild-type mice (**b** and **d**). (**a** and **b**) NKCC1 single staining; (**c** and b) Stat5a single staining; (**a′**–**d′**) β-catenin single staining; (**a″**–**d″**) merged staining of NKCC1 or Stat5a with β-catenin. Note: Although NKCC1 and Stat5a were expressed uniformly in wild-type prostate epithelium (**b** and **d**), it was absent in cells that accumulated β-catenin (**a** and **c**)

Stat5a expression (Figure 5c, c′ and c″) while homogeneous nuclear staining was observed in wild-type prostate epithelium (Figure 5d, d′ and d″). Collectively, these findings suggest that the initial β-catenin stabilization results in the loss of normal prostate epithelial characteristics followed by the formation of hyperplasias and transdifferentiation into squamous metaplasias.

Neoplastic progression of mutant prostate epithelium upon transplantation

MMTV-Cre-mediated activation of β-catenin also resulted in severe skin lesions and mice had to be killed no later than 3 months of age. Thus it was not possible to investigate the temporal progression of the hyperplasias and metaplasias. In addition, this model did not permit a distinction of systemic and cell autonomous effects. To overcome these obstacles, ventral prostate tissue from 9-week-old mutant mice ($Catnb^{+/\Delta ex3}$:$MMTV^{cre}$ and $Catnb^{+/\Delta ex3}$) was transplanted into cleared mammary fat pads of 3-week-old wild-type males. This permitted the evaluation of the consequences of activated β-catenin at later timepoints. After the transplantation, mutant and control tissues were maintained for an additional 9 weeks before they were harvested (Figure 6a–c), which equaled a combined time of β-catenin stabilization of 18 weeks. Transplanted prostate tissue from control animals formed intact alveolar structures with open lumina (Figure 6c and f). In contrast to the controls, the $Catnb^{+/\Delta ex3}$:$MMTV^{cre}$ transplants had a thick encapsulation that surrounded the prostatic epithelium (Figure 6a and b). There were four types of morphological identities adopted by the encapsulated mutant prostatic tissues. The first morphological identity was a normal single cell layer surrounding a lumen (data not shown), the second morphology were small hyperplastic nodules that extended into the lumen from the alveolar surface (data not shown), the third identity was an accumulation of large intra-acinous hyperplastic nodules that extended into the lumen (Figure 6d), and the last was the filled lumen consisting of hyperplastic epithelial cells with circular occlusions and occasional keratin deposits (Figure 6e). The hyperplastic nodules in the $Catnb^{+/\Delta ex3}$:$MMTV^{cre}$ transplants demonstrated high levels of β-catenin accumulation (Figure 6g, j, m and p). Keratin 5 expression was not altered (Figure 6h), but NKCC1 expression was dramatically decreased in the areas of β-catenin accumulation (Figure 6k). Interestingly, expression of keratins 1 and 6 in the transplants was low (Figure 6n and q, respectively). The decrease of keratins 1 and 6 in the prostate after transplantation suggests a dominance of hyperproliferation over squamous metaplasia formation upon extended accumulation of β-catenin.

Stabilized β*-catenin induces epithelial hyperplasias in the vas deferens, epididymis, coagulating gland, seminal vesicle and salivary gland*

As shown in Figure 1, stabilized β-catenin was also detected in the vas deferens, epididymis, coagulating gland, salivary gland and seminal vesicle. Although the overall histological appearance of these organs from 8-week-old mice was normal (Figure 7a–e), immunohistochemical analyses revealed areas containing excessive β-catenin accumulation. In addition, cells in these areas had undergone proliferation and were positive for keratin 5 (Figure 7a″–e″). Interestingly, and unlike the prostate, no keratin 1 or keratin 6 expression was observed in these tissues from $Catnb^{+/\Delta ex3}$:$MMTV^{cre}$ or wild-type mice (data not shown). It is not clear at this point whether these lesions may continue to proliferate and undergo transdifferentiation at a later timepoint. Stabilization of β-catenin in epithelial cells of the preputial gland resulted in a complete squamous transdifferentiation by 12 weeks of age (Figure 2f).

Stabilization of β*-catenin in prostate epithelium leads to the activation of matrix metalloproteinase 9 (MMP9)*

The presence of areas containing hyperplasias and squamous metaplasias suggested the occurrence of tissue remodeling. To investigate the nature of remodeling during the transdifferentiation process, the activity of metalloproteinases was monitored in zymogram gels (Figure 8). Strong activation of MMP9 was detected in the ventral prostate from $Catnb^{+/\Delta ex3}$:$MMTV^{cre}$ mice, where hyperplasias and squamous transdifferentiation of epithelial cells had been observed. In contrast to MMP9, we observed no difference in MMP2 activity, and this would suggest that rather than secretion by inflammatory cell types, the altered MMP9 expression is due to the stabilization of β-catenin. The presence of increased MMP9 activity in the prostate from $Catnb^{+/\Delta ex3}$:$MMTV^{cre}$ mice may indicate an elevated potential for the expansion of hyperplastic areas. Further, the overexpression of active MMP9 has been linked to several tumor models (Baruch *et al*., 2001; Kallakury *et al*., 2001; Rodriguez-Manzaneque *et al*., 2001), and this enzymatic activity may confer another growth advantage to an expanding population of squamous metaplastic or neoplastic cell types in vivo.

Discussion

Wnt/β-catenin signaling is involved in cell fate determination (Huelsken and Birchmeier, 2001) and activation of this pathway can result in the transdifferentiation of one cell type into an unrelated one, as demonstrated by our previous work in the mammary gland (Miyoshi *et al*., 2002a and c). While the ectopic expression of stabilized β-catenin in the basal cells of the skin promotes de novo formation of hair follicles (Gat *et al*., 1998), the inhibition of this pathway leads to conversion of hair follicles into interfollicular epidermis (Niemann *et al*., 2002). In addition, the loss of β-catenin results in the establishment of cysts and progressive hair loss (Huelsken *et al*., 2001).

The current work demonstrates that the activation of β-catenin signaling in prostate epithelium led to hyperplasias and transdifferentiation into squamous

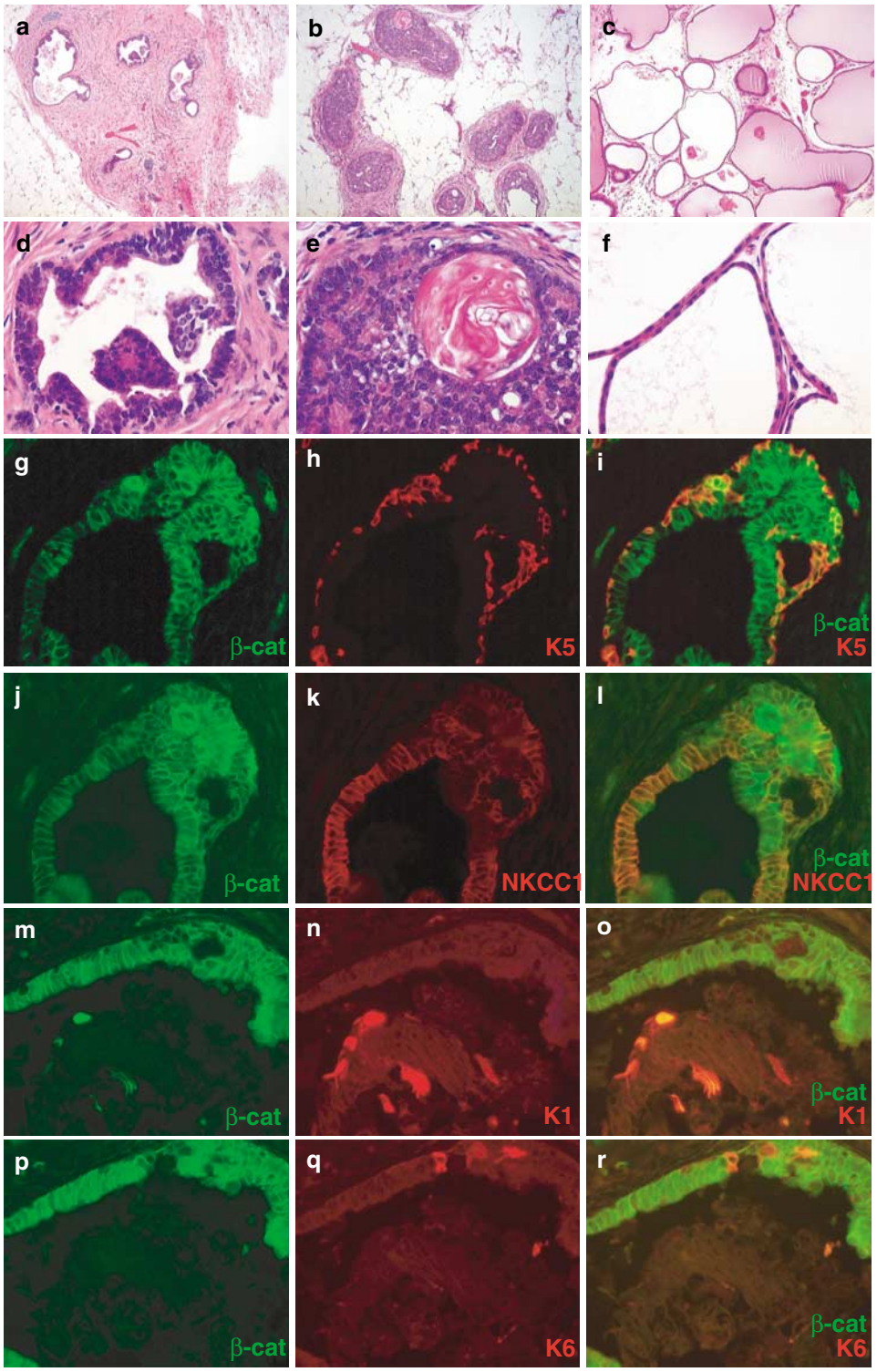

Figure 6 Transplants from *Catnb*$^{+/\Delta ex3}$*:MMTV*^{cre} prostate tissues demonstrate the preferential enrichment of hyperplastic intra-acinous growth over squamous transdifferentiation. H&E staining from transplanted *Catnb*$^{+/\Delta ex3}$*:MMTV*^{cre} and *Catnb*$^{+/\Delta ex3}$ ventral prostate tissues in the cleared stromal compartment of the male mammary gland (**a**–**f**). The *Catnb*$^{+/\Delta ex3}$*:MMTV*^{cre} prostates displayed numerous foci of intra-acinous hyperplasia and areas of filled lumina surrounded by a relatively thick encapsulation (**a** and **b**, **d** and **e**). The control transplants displayed a morphology that was similar to the endogenous ventral prostate (**c** and **f**). Markers keratin 5 and NKCC1 demonstrated similar expression to the endogenous mutant prostate (**h** and **k**, respectively). The expression of keratin 1 and keratin 6 was altered (**n** and **q**, respectively) from the endogenous mutant glands when compared to tissues from 7.5 to 12 weeks of age. The dominant signal from keratin 1 (**n**) occurred in the centriacinar keratin deposits, but some of the cells continued to produce this marker (data not shown). β-Catenin (**g**, **j**, **m** and **p**) was separated from each merged image (**i, l, o** and **r**) to show the individual contribution for each marker

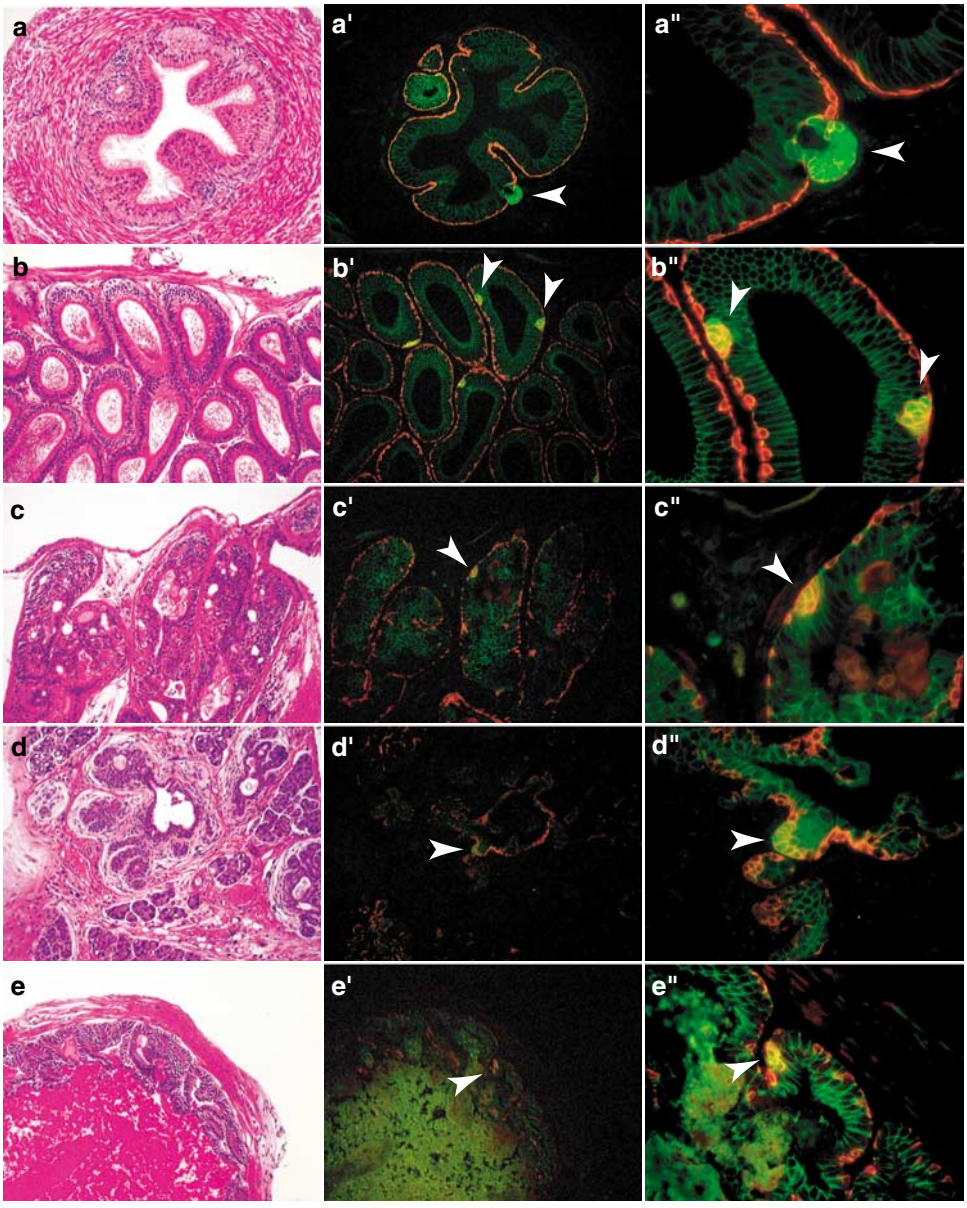

Figure 7 Analysis of the vas deferens, epididymis, coagulating gland, salivary gland and seminal vesicle. H&E staining of the vas deferens (**a**), epididymis (**b**), coagulating gland (**c**), salivary tissue (**d**) and seminal vesicle (**e**) from 8-week-old $Catnb^{+/\Delta ex3}$:$MMTV^{cre}$ mice. Overall histological appearance was normal in each tissue. (**a**′–**e**′) Immunohistochemistry of β-catenin and keratin 5 in serial sections from (**a**–**e**), respectively. (**a**″–**e**″) Higher magnification of (**a**′–**d**′), respectively. Note: Sporadic hyperplastic lesions expressing accumulated β-catenin (**a**′–**e**′ and **a**″–**e**″, arrowheads). Magnification: (**a**–**e**) and (**a**′–**e**′), ×200; (**a**″–**e**″), ×630

metaplasias. These cells displayed features reminiscent of interfollicular epidermis and hyperproliferative interfollicular epidermis. The acquisition of epidermal characteristics coincided with the cell-specific loss of NKCC1 and nuclear Stat5, which are features of normal differentiated prostate and mammary epithelia. The changes in NKCC1, Stat5a and K5 expression are located in cells within lesions that are associated with β-catenin overexpression. However, these cells do not necessarily exhibit high levels of β-catenin at the time the tissue was harvested and prepared for immunostaining. This may be the result of cell cycle-associated fluctuations in β-catenin levels, or a reduction of β-catenin levels once the cellular phenotype has been altered towards hyperplasias and metaplasias. This study demonstrates that functional prostate epithelium has the capacity to adopt a differentiation program that is unrelated to the lineage it is derived from. The plasticity of epidermal stem cells has been recognized (Gat *et al*., 1998; Watt and Hogan, 2000; Merrill *et al*., 2001), and there are examples that the fate of neuronal and hematopoietic cells can be diverted even after the establishment of particular programs of differentiation (Kondo *et al*., 2000; Ross *et al*., 2000). In the prostate, such reprogramming of cells can be facilitated simply through the prolonged induction of β-catenin. Therefore

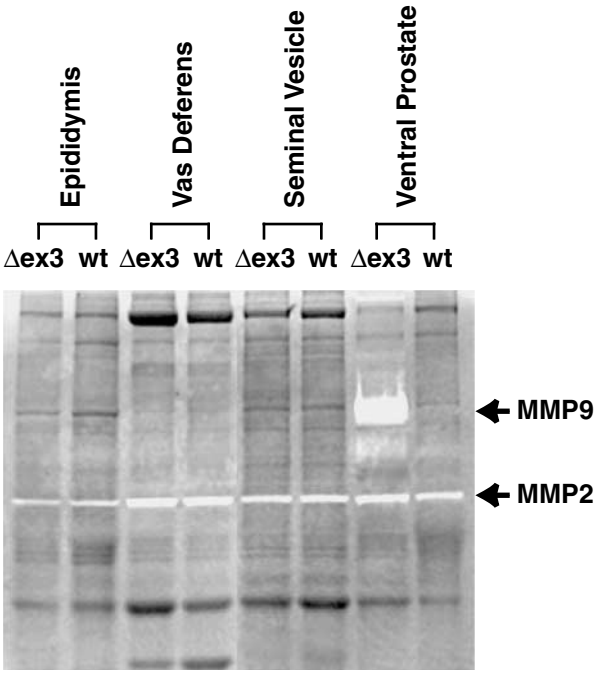

Figure 8 Matrix metalloproteinase 9 MMP9 was highly induced in ventral prostate of mutant mice. MMP activity was analysed by zymogram in epididymis, vas deferens, seminal vesicle and prostate from 8-week-old $Catnb^{+/\Delta ex3}$:$MMTV^{cre}$ and wild-type mice. Note: The strong activation of MMP9 was detected in the ventral prostate from $Catnb^{+/\Delta ex3}$:$MMTV^{cre}$ mice. Δex3, $Catnb^{+/\Delta ex3}$:$MMTV^{cre}$; wt, wild type. MMP2 activity does not seem to be altered in any of the mutant or $Catnb^{+/\Delta ex3}$:$MMTV^{cre}$ or $Catnb^{+/\Delta ex3}$ sample

it appears that Wnt/β-catenin signaling is dominant even over existing differentiation programs initiated in both mammary and prostate epithelium. However, the extent to which β-catenin signaling can induce proliferation and transdifferentiation is cell-specific. Thus while the stabilization of β-catenin in mammary epithelium leads almost exclusively to the formation of squamous metaplasia (Miyoshi *et al*., 2002a), both hyperplasias and squamous metaplasias were observed in the prostate as shown here. In contrast, adenomatous polyps were observed in the intestine (Harada *et al*., 1999). The lack of observable neoplasias and tumors in hepatocytes expressing a stabilized β-catenin (Harada *et al*., 2002) further supports the concept of the cell-specific nature of β-catenin signaling.

Recently, Gounari *et al*. (2002) reported the extensive presence of high-grade PIN-like lesions in mouse prostate epithelium upon the stabilization of β-catenin. This observation is in contrast to the current study in which we failed to find evidence of such lesions in a total of eight mice, which ranged in age between 8 and 12 weeks. Although it appears unlikely that strain differences can account for such variability given that the source of the β-catenin mice and MMTV-Cre mice was the same, subtleties in strain background cannot be ruled out. One possible explanation for the differences could be the duration of β-catenin activation and possible secondary effects. While predominantly squamous metaplasias were observed in 8–12-week-old mice, Gounari observed high-grade PIN-like lesions in mice ranging from 10 to 21 weeks of age. MMTV-Cre-mediated deletion of exon 3 of the β-catenin gene occurs not only in mammary and prostate epithelia but also in a number of other cell types, including skin and immune cells. The physiological consequences are profound and we had to kill the mice at 3 months of age. A transplantation approach permitted the evaluation of long-term consequences of β-catenin activation in the absence of systemic effects. Under these experimental conditions hyperplasias, possible neoplasias and squamous metaplasias were detected. This observation suggests that the cumulative activation of β-catenin can lead to distinct cellular lesions. We therefore hypothesize that an early event is the transdifferentiation of prostate epithelium into squamous metaplasias. However, cells, which escape the transdifferentiation process, can progress into intra-acinous hyperplasias with the possibility of neoplastic transformation.

The development of squamous metaplasias from endoderm-derived cells implies an erasure of several steps of developmental commitment, but the cell-specific executors of this conversion remain to be defined. The gene discovery efforts emerging from this study might provide information on mechanisms that result in the loss of differentiation and the acquisition of an epidermal fate. We identified known and unknown genes with increased levels of expression in the transdifferentiated prostate. Some of these genes were also induced in transdifferentiated mammary tissue, further supporting the notion that activated β-catenin induces an epidermal fate in both cell types. Among the genes activated in transformed prostate tissue were those encoding lactotransferrin, SPRR2A, NET1 and APLP2. High levels of lactotransferrin have been detected in neoplastic cells and differentiated adenocarcinomas of the prostate, but not in undifferentiated carcinomas (Barresi and Tuccari, 1984). Since lactotransferrin levels are increased upon inflammation of the human prostate gland (Reese *et al*., 1992) and high levels are detected in lymphocytes, it is possible that the expression in prostate tissue upon β-catenin stabilization reflects both hyperplasias and an immune response. It is worth noting that other genes linked to immune cell activity are also activated, including the lymphocyte antigen 6 complex and WM65 κ-immunoglobulin (Table 1). SPRR2A is a member of the cornified cell envelope precursors in the same subclass as loricrin, involucrin and the other SPRRs (Fischer *et al*., 1998). The expression of SPRR2A is confined to squamous and glandular epithelia such as the mammary gland, prostate, salivary gland and kidney (Oettgen *et al*., 1999). In addition, SPRR2A has been associated with terminal keratinocyte differentiation, and its regulation may be coordinated with other genes such as profilaggrin in forming the epidermal differentiation complex (Fischer *et al*., 1998). SPRR2A is a structural component of the cornified cell envelope of squamous epithelia (Song *et al*., 1999) and the increased levels observed in mutant prostate further support the notion that the epithelium had undergone a

transdifferentiation process. NET1, a guanine exchange factor that is able to activate RhoA (Alberts and Treisman, 1998), is an important mediator of stress fiber formation in TGFβ-mediated signaling (Shen *et al*., 2001). TGFβ has been shown to induce NET1 expression (Shen *et al*., 2001) and its levels were induced within 48 h after β-catenin activation. Thus, the early induction of TGFβ may infer the effects of an activated downstream signal during the initial stages of β-catenin accumulation. Lastly, APLP2 is a ubiquitously expressed secreted protein (Slunt *et al*., 1994), which has been implicated in cell motility toward fibronectin and collagen with an increase in the affinity to bind these substrates (Li *et al*., 1999).

In summary, by 8 weeks of age the activation of β-catenin has resulted in diffuse hyperplasia of the prostate and submucosal glands of the urethra with extensive squamous metaplasias that produce cellular hard keratins. This pattern is strikingly similar to that seen upon stabilization of β-catenin in mouse mammary tissue (Miyoshi *et al*., 2002a). Subsequent transplantation of transformed prostate tissue into a wild-type host resulted in the development of hyperplastic and possible neoplastic foci as well as squamous metaplasia after an additional 2 months. These results suggest that the activation of β-catenin leads to progressive cellular changes, which includes hyperplasias, squamous metaplasias and a subsequent shift toward neoplastic transformation.

Materials and methods

Generation of constitutively active β*-catenin*

The floxed β-catenin mice and MMTV-Cre transgenic mice have been described (Wagner *et al*., 1997; Harada *et al*., 1999). Mice containing one wild-type β-catenin allele and one conditional allele ($Catnb^{+/lox(ex3)}$) were mated with the MMTV-Cre mice to generate $Catnb^{+/lox(ex3)}$:Tg:$MMTV^{cre}$ mice (referred to as $Catnb^{+/\Delta ex3}$:$MMTV^{cre}$ mice).

Western blotting

Protein was isolated from each tissue as previously described (Liu *et al*., 1996). A total of 40 μg of protein was separated by electrophoresis in Tris–glycine gels (Invitrogen, Carlsbad, CA, USA). Membranes were blocked overnight at 4°C in TBST (Tris-buffered saline. pH 7.4, with 0.05% Tween 20) containing 5% (wt/vol) nonfat dried milk. Primary mouse monoclonal anti-β-catenin (Transduction Laboratories, Lexington, KY, USA) was applied at 1 : 1000 and incubated with the membranes for 1 h at room temperature. Subsequently, membranes were incubated with a horseradish peroxidase (HRP)-linked anti-mouse antibody for 30 min at room temperature. Specifically bound secondary antibodies were visualized using an enhanced chemiluminescence procedure (Pierce Chemical, Rockford, IL, USA).

Histology and immunohistochemistry

Each tissue was isolated from $Catnb^{+/\Delta ex3}$:$MMTV^{cre}$ mice and fixed in Telly's fixative for 4 h. After fixation, samples were dehydrated, embedded in paraffin and sectioned at 5 μm. For histology, sections were stained with hematoxylin and eosin. For immunohistochemistry, the primary antibodies were obtained from the following sources: rabbit polyclonal anti-Stat5a (Liu *et al*., 1996), rabbit polyclonal anti-keratin 1 (Babco. Richmond, CA, USA), rabbit polyclonal anti-keratin 5 (Babco) and rabbit polyclonal anti-keratin 6 (Babco). To detect the primary antibodies fluorochrome conjugated anti-mouse (Alexafluor 488) and fluorochrome conjugated anti-rabbit (Alexafluor 594) secondary antibodies (Molecular Probes) were used for immunohistochemistry. The primary antibodies (keratin 1, 1 : 200; keratin 5, 1 : 200; keratin 6, 1 : 200; β-catenin, 1 : 100; NKCC1, 1 : 1000; Stat5a, 1 : 600) were applied to the sections and incubated at 37°C for 1 h. Sections were subsequently incubated with fluorescent-conjugated anti-mouse and anti-rabbit secondary antibodies at 37°C for 1 h. An HRP-conjugated anti-rabbit antibody was used for the detection of rabbit polyclonal anti-involucrin (Babco 1 : 1000), rabbit polyclonal antiloricrin (Babco, 1 : 500), and rabbit polyclonal antifilaggrin (Babco, 1 : 1000) using an appropriate ABC kit (Vector Laboratories, Inc., Burlingame, CA, USA) following the manufacturer's protocol. To visualize the bound antibodies, we used a DAB kit (Vector Laboratories, Inc., Burlingame, CA, USA) as described by the manufacturer's protocol excluding addition of the nickel substrate. The slides were counterstained with hematoxylin, dehydrated and mounted using Permount (Fisher Scientific).

Microarray analysis

The microarray analyses were performed with a 12.6k containing cDNAs from the NCI oncochip (GEM1) and from the mammochip (Miyoshi *et al*., 2002b). RNA was prepared from prostates of four 8-week-old transgenic mice and four control littermates using TRIzol extraction (Life Technologies, Rockville, MD, USA) followed by two ethanol precipitations. RNA from the four mice was pooled for the array analysis. From the MEF cultures, three individual plates were pooled for RNA in each of two replicate experiments. RNA was then prepared from the individual pools using TRIzol followed by two ethanol washes. For fluorescence labeling, 20 μg of total RNA were reverse transcribed in presence of 300 U of SS II (Life Technologies, Rockville, MD, USA) and labeled with cy3-dUTP and cy5-dUTP (MEN, Boston, MA, USA). Samples were combined, purified and concentrated with YM30 Microcon columns (Millipore, Bedford, MA, USA). Slides were prehybridized for 1 h and hybridized overnight at 42°C, in 25% formamide. Slides were washed in 2 × SSC/0.1% SDS 4′, 1 × SSC 4′, 0.2 × SSC 4′, 0.05 × SSC 1′, dried by centrifugation, and scanned on a GenePix 4000A scanner (Axon Instruments, Foster City, CA, USA). The images were analysed by GenePix Pro 3.0 (Axon Instruments, Foster City, CA, USA). Each experiment was repeated with switching the labeling. The data were deposited in the NCI-CIT microarray database and normalized data were analysed with the included 'mAdb tools' with some modifications: the differentially expressed genes were selected by signal intensity of fivefold over the average slide background in at least one channel and an expression ratio of 3/0.3 or higher. These criteria had to be met also in the reverse-labeled experiments.

Northern blot analysis

RNA preparation has been described in the microarray section, and 20 μg of total RNA was loaded for each sample. The Northern blots were performed as described previously (Robinson *et al*., 1995). Primers for cDNA probes were produced as purified PCR fragments from the following

primers: LTF F-5′CCGCTCAGTTGTGTCAAGAA3′ LTF R-CTGCTTGCTCTGTTCCACTG3′; SPRR2A F-5′TCCGGAGAACCTGATTCTGA3′ SPRR2A R-AGGTAACAGGCAGGCTGAGA3′; NET1 F-5′GCAGCCTTGATTTGAAGGAG3′ NET1 R-CCGAGTCCAAACCAAGATGT3′; APLP2 F-5′ACCTGGAGCAGATGCAGATT3′ APLP2 R-5′TCATGCACAACCCAGAACAT3′; GAPDH F-5′GTGAAGGTCGGTGTGAACGGATTTGGCCGT3′-F GAPDH R-5′CCACCACCCTGTTGCTGTAG3′-R. All of the probes were sequenced prior to hybridization to ensure accuracy of the PCR fragment.

MEF preparation and Cre excision in vitro

MEFs were derived from 14-day-old embryos with the genotype of $Catnb^{+/\Delta ex3}$. The 14-day-old embryos were isolated, the heads were removed and the liver was removed with the other internal organs. The remaining tissue for each embryo was placed in 1 ml of trypsin/EDTA (Gibco) mashed briefly with a pipette tip and incubated for 10 min at 37°C. A volume of 10 ml of MEF medium (DMEM 500 ml (Gibco), penicillin + streptomycin 3 ml (Gibco), nonessential amino acids 6 ml (Gibco), L-glutamine 10 ml (Gibco), fetal calf serum 90 ml (Gibco), 2-mercaptoethanol 4 μl (Sigma)) was added to the tissue, triturated with a pipette tip and plated on 10 cm culture dishes. After overnight incubation at 37°C in 5% CO_2, the medium was changed and the cells were passed the following day. After the cells had reached 50% confluence, they were infected with a pBabe retro-Cre construct (Krempler *et al*., 2002) in the presence of 1 mg/ml polybrene with a volume of 4 ml MEF medium. After the initial incubation, 1 ml of the same virus solution was added and incubated for 2 h. Finally, the last 1 ml of virus was added to the plate and incubated for 2 h. A volume of 6 ml of MEF medium was added to each dish and incubated overnight. The next day the medium was aspirated and 10 ml of fresh MEF medium was added to each plate then allowed to incubate overnight. Puromycin (Sigma) was used at 2.5 μg/ml in MEF medium for a selection lasting 18 h. After selection, the cells were collected for protein and RNA analysis. Deletion efficiency was visualized by the appearance of a truncated β-catenin protein by Western blot.

Transplantation of prostate tissues

The recipients were athymic nude mice that had been kept in a sterile facility. The mammary fat pad was cleared at 3 weeks of age (DeOme *et al*., 1959). The fourth and fifth inguinal glands were separated by cauterization, and the blood supply to the fourth gland was also cauterized below the lymph node before excision of the tissue from the nipple to the lymph node. The nipple was then cauterized from the inside to ensure that no new epithelial growth could occur. All excised tissues were kept and analysed to ensure that all of the epithelium had been cleared (after a standard whole-mount stain using carmine alum). The donor tissues were collected from $Catnb^{+/\Delta ex3}$ and $Catnb^{+/\Delta ex3}$:$MMTV^{cre}$ littermates at 9 weeks of age. The ventral prostate was excised and placed into 1 × PBS. Prostate tissues were minced into small pieces (about 1 mm^3) and then surgically inserted into the fourth inguinal gland of the recipient through a small incision in the fat pad. In order to minimize small systemic variations in the different recipients, each host had both a control and contralateral mutant transplant. The mammary fat pads were collected after 9 weeks of growth within the recipients. The tissues were then fixed and stained using the same protocols as the endogenous glands stated in the Histology and immunohistochemistry section.

Zymogram gel analysis

Coomassie-stained casein and gelatin zymogram SDS-PAGE were carried out essentially as described in the manufacturer's protocol (Invitrogen, Carlsbad, CA, USA). The lysate was loaded with 40 μg of protein per well. Zymography was carried out on gelatin-embedded 10% Tris–glycine gels (Invitrogen, Carlsbad, CA, USA). The gel was fixed after zymogram developing for 2 h in 50% methanol, 10% acetic acid, stained overnight in 50% methanol, 0.05% brilliant cresyl blue, and destained in 5% methanol, 7% acetic acid until the background cleared. The gel was dried according to the manufacturer's protocol (Research Products International Corporation, Mount Prospect, IL, USA).

Abbreviations

EST, expressed sequence tag; LTR, long terminal repeat; MMP, matrix metalloproteinase; MMTV, mouse mammary tumor virus; Stat, signal transducer and activator of transcription.

Acknowledgements

We acknowledge N Harada, who originally generated the floxed mice. Part of this work was supported by grants from the Ministry of Education, Science, Sports and Culture, Japan; and Organization for Pharmaceutical Safety and Research, Japan. The rabbit polyclonal NKCC1 antibody that has been previously described (Moore-Hoon and Turner, 1998), was a kind gift from Dr Jim Turner, National Institute of Craniofacial and Dental Research, NIH (Bethesda, MD, USA).

References

Achtstatter T, Moll R, Moore B and Franke WW. (1985). *J. Histochem. Cytochem.*, **33,** 415–426.
Alberts AS and Treisman R. (1998). *EMBO J.*, **17,** 4075–4085.
Barresi G and Tuccari G. (1984). *Virchows Arch. A.*, **403,** 59–66.
Baruch RR, Melinscak H, Lo J, Liu Y, Yeung O and Hurta RA. (2001). *Cell Biol. Int.*, **25,** 411–420.
Brault V, Moore R, Kutsch S, Ishibashi M, Rowitch DH, McMahon AP, Sommer L, Boussadia O and Kemler R. (2001). *Development*, **128**, 1253–1264.
Chesire DR, Ewing CM, Gage WR and Isaacs WB. (2002). *Oncogene*, **21,** 2679–2694.
Chesire DR, Ewing CM, Sauvageot J, Bova GS and Isaacs WB. (2000). *Prostate*, **45,** 323–334.
de Lau W and Clevers H. (2001). *Nat. Genet.*, **28,** 3–4.
DeOme KB, Faulkin Jr LJ, Bern HA and Blair PE. (1959). *Cancer Res.*, **19,** 515–520.
Fischer DF, van Drunen CM, Winkler GS, van de Putte P and Backendorf C. (1998). *Nucleic Acids Res.*, **26,** 5288–5294.
Fuchs E and Byrne C. (1994). *Curr. Opin. Genet. Dev.*, **4,** 725–736.
Gat U, DasGupta R, Degenstein L and Fuchs E. (1998). *Cell*, **95,** 605–614.

Gerstein AV, Almeida TA, Zhao G, Chess E, Shih Ie M, Buhler K, Pienta K, Rubin MA, Vessella R and Papadopoulos N. (2002). *Genes Chromosomes Cancer*, **34,** 9–16.

Gounari F, Signoretti S, Bronson R, Klein L, Sellers WR, Kum J, Siermann A, Taketo MM, von Boehmer H and Khazaie K. (2002). *Oncogene*, **21,** 4099–4107.

Haegel H, Larue L, Ohsugi M, Fedorov L, Herrenknecht K and Kemler R. (1995). *Development*, **121,** 3529–3537.

Harada N, Miyoshi H, Murai N, Oshima H, Tamai Y, Oshima M and Taketo MM. (2002). *Cancer Res.*, **62,** 1971–1977.

Harada N, Tamai Y, Ishikawa T, Sauer B, Takaku K, Oshima M and Taketo MM. (1999). *EMBO J.*, **18,** 5931–5942.

Hovanes K, Li TW, Munguia JE, Truong T, Milovanovic T, Lawrence Marsh J, Holcombe RF and Waterman ML. (2001). *Nat. Genet.*, **28,** 53–57.

Huelsken J and Birchmeier W. (2001). *Curr. Opin. Genet. Dev.*, **11,** 547–553.

Huelsken J, Vogel R, Brinkmann V, Erdmann B, Birchmeier C and Birchmeier W. (2000). *J. Cell Biol.*, **148,** 567–578.

Huelsken J, Vogel R, Erdmann B, Cotsarelis G and Birchmeier W. (2001). *Cell*, **105,** 533–545.

Humphreys RC and Hennighausen L. (1999). *Cell Growth Differ.*, **10,** 685–694.

Kallakury BV, Karikehalli S, Haholu A, Sheehan CE, Azumi N and Ross JS. (2001). *Clin. Cancer Res.*, **7,** 3113–3119.

Kondo M, Scherer DC, Miyamoto T, King AG, Akashi K, Sugamura K and Weissman IL (2000). *Nature*, **407,** 383–386.

Krempler A, Henry MD, Triplet AA and Wagner KU. (2002). *J. Biol. Chem.*, **277,** 43216–43223.

Li XF, Thinakaran G, Sisodia SS and Yu FS. (1999). *J. Biol. Chem.*, **274,** 27249–27256.

Liu X, Robinson GW and Hennighausen L. (1996). *Mol. Endocrinol.*, **10,** 1496–1506.

Liu X, Robinson GW, Wagner KU, Garrett L, Wynshaw-Boris A and Hennighausen L. (1997). *Genes Dev.*, **11,** 179–186.

McCrea PD, Turck CW and Gumbiner B. (1991). *Science*, **254,** 1359–1361.

Merrill BJ, Gat U, DasGupta R and Fuchs E. (2001). *Genes Dev.*, **15,** 1688–1705.

Miyoshi K, Shillingford JM, Smith GH, Grimm SL, Wagner KU, Oka T, Rosen JM, Robinson GW and Hennighausen, L. (2001). *J. Cell Biol.*, **155,** 531–542.

Miyoshi K, Meyer B, Gruss P, Cui Y, Renou JP, Morgan FV, Smith GH, Reichenstein M, Shani, M and Hennighausen, L and Robinson, GW. (2002b). *Mol. Endocrinol.*, **16,** 2892–2901.

Miyoshi K, Rosner A, Nozawa M, Byrd C, Morgan F, Landesman-Bollag E, Xu X, Seldin DC, Schmidt EV, Taketo MM, Robinson GW, Cardiff RD and Hennighausen L. (2000c). *Oncogene*, **21,** 5548–5556.

Miyoshi K, Shillingford JM, Le Provost F, Gounari F, Bronson R, von Boehmer H, Taketo MM, Cardiff RD, Hennighausen L and Khazaie K. (2002a). *Proc. Natl. Acad. Sci. USA*, **99,** 219–224.

Nevalainen MT, Ahonen TJ, Yamashita H, Chandrashekar V, Bartke A, Grimley PM, Robinson GW, Hennighausen L and Rui H. (2000). *Lab. Invest.*, **80,** 993–1006.

Niemann C, Owens DM, Hulsken J, Birchmeier W and Watt PM. (2002). *Development*, **129,** 95–109.

Oettgen P, Kas K, Dube A, Gu X, Grall F, Thamrongsak U, Akbarali Y, Finger E, Boltax J, Endress G, Munger K, Kunsch C and Libermann TA. (1999). *J. Biol. Client.*, **274,** 29439–29452.

Polakis P. (2000). *Genes Dev.*, **14,** 1837–1851.

Reese JH, McNeal JE, Goldenberg SL, Redwine EA and Sellers RG. (1992). *Prostate*, **20,** 73–85.

Robinson GW, McKnight RA, Smith GH, Hennighausen L. (1995). *Development*, **121,** 2079–2090.

Rodriguez-Manzaneque JC, Lane TF, Ortega MA, Hynes RO, Lawler J and Iruela-Arispe ML. (2001). *Proc. Natl. Acad. Sci. USA*, **98,** 12485–12490.

Roose J, Huls G, van Beest M, Moerer P, van der Horn K, Goldschmeding R, Logtenberg T and Clevers H. (1999). *Science*, **285,** 1923–1926.

Ross SE, Hemati N, Longo KA, Bennett CN, Lucas PC, Erickson RL and MacDougald OA (2000). *Science*, **289,** 950–953.

Shen X, Li J, Hu PP, Waddell D, Zhang J and Wang XF. (2001). *J. Biol. Chem.*, **276,** 15362–15368.

Shillingford JM, Miyoshi K, Flagella M, Shull GE and Hennighausen L. (2002a). *Mol. Endocrinol.*, **16,** 1309–1321.

Shillingford JM, Miyoshi K, Robinson GW, Grimm SL, Rosen JM, Neubauer H, Pfeffer K and Hennighausen L. (2002b). *Mol. Endocrinol.*, **16,** 563–570.

Slunt HH, Thinakaran G, Von Koch C, Lo AC, Tanzi RE and Sisodia, SS. (1994). *J. Biol. Chem.*, **269,** 2637–2644.

Song HJ, Poy G, Darwiche N, Lichti U, Kuroki T, Steinert PM and Kartasova T (1999). *Genomics*, **55,** 28–42.

Voeller HJ, Truica CI and Gelmann EP. (1998). *Cancer Res.*, **58,** 2520–2523.

Wagner KU, McAllister K, Ward T, Davis B, Wiseman R and Hennighausen L (2001). *Transgenic Res.*, **10,** 545–553.

Wagner KU, Wall RJ, St-Onge L, Gruss P, Wynshaw-Boris A, Garrett L, Li M, Furth PA and Hennighausen L. (1997). *Nucleic Acids Res.*, **25,** 4323–4330.

Watt FM and Hogan BL. (2000). *Science*, **287,** 1427–1430.

Widelitz RB, Jiang TX, Lu J and Chuong CM. (2000). *Dev. Biol.*, **219,** 98–114.